Chem. Commun., 649 (1971); A. Kalman, K. Sasvari, and I. Kapovits, *Acta Crystallogr., Sect. B*, **29**, 335 (1971). (b) $(C_6H_5)_2S(OC(CF_3)_2C_6H_5)_2$: I. C. Paul, J. C. Martin, and E. F. Perozzi, *J. Am. Chem. Soc.*, **93**, 6674 (1971); *ibid.*, **94**, 5010 (1972). (c) $Cl_2S(C_6H_4Cl)_2$: N. C. Baenziger, R. E. Buckles, R. J. Maner, and T. D. Simpson, *ibid.*, **91**, 5749 (1969). (d) $Cl_2Se(C_6H_5)_2$ and $Br_2Se(C_6H_5)_2$: J. D. McCullough and G. Hamburger, *ibid.*, **64**, 508 (1942). (e) $Cl_2Se(p\text{-}C_6H_4CH_3)_2$ and $Br_2Se(p\text{-}C_6H_4CH_3)_2$: J. D. McCullough and R. E. Marsh, *Acta Crystallogr.*, **3**, 41 (1950). (f) $TeCl_4$: D. P. Stevenson and V. Schomaker, *J. Am. Chem. Soc.*, **62**, 1267 (1940). (g) $Br_2Te(C_6H_5)_2$: G. D. Christofferson and J. D. McCullough, *Acta Crystallogr.*, 11, 249 (1958). (h) $I_2Te(p\text{-}C_6H_4Cl)_2$: G. Y. Chao and J. D. McCullough, *ibid.*, **15**, 687 (1962). (i) $Cl_2Te(CH_3)_2$: G. D. Christofferson, R. A. Sparks, and J. D. McCullough, *ibid.*, 11, 782 (1958). (j) $I_2Te(C_{12}H_6O)$: J. D. McCullough, *Inorg. Chem.*, **12**, 2669 (1973). (k) $I_2Te(C_{12}H_8)$: J. D. McCullough, *ibid.*, **14**, 1142 (1975). (l) $I_2Te(C_4H_8O)$: H. Hope, C. Knobler, and J. D. McCullough, *ibid.*, **12**, 2665 (1973). (m) $I_2Te(C_4H_8S)$: C. Knobler, J. D. McCullough, and H. Hope, *ibid.*, **9**, 797 (1970). (n) $Br_2Se(C_4H_8S)$: L. Batelle, C. Knobler, and J. D. McCullough, *ibid.*, **6**, 958 (1967). (o) $Cl_2SeC_4H_8SeCl_2$: A. Amendola, E. S. Gould, and B. Post, *ibid.*, **3**, 1199 (1964). (p) $Br_2Te(C_4H_8S)$: C. Knobler and J. D. McCullough, *ibid.*, 11, 3026 (1972).

(3) E. L. Muetterties and R. A. Schunn, *Q. Rev., Chem. Soc.*, **20**, 245 (1966).

(4) This is discussed in many of the structural papers in ref 2. For example in $Br_2Se(C_6H_5)_2$ the axial Se–Br bonds are 2.52 (1) Å while the sum of the covalent radii is only 1.17 + 1.14 = 2.31 Å. In contrast the equatorial Se–C bonds are normal, 1.91 (3) Å compared with the sum of the covalent radii of 1.17 + 0.772 = 1.94 Å.

(5) (a) R. J. Hach and R. E. Rundle, *J. Am. Chem. Soc.*, **73**, 4321 (1951); R. E. Rundle, *ibid.*, **85**, 112 (1963); R. E. Rundle, *Surv. Prog. Chem.*, 1, 81 (1963); (b) G. C. Pimentel, *J. Chem. Phys.*, **19**, 446 (1951); (c) E. E. Havinga and E. H. Wiebenga, *Recl. Trav. Chim. Pays-Bas*, **78**, 724 (1959); (d) R. J. Gillespie, *Inorg. Chem.*, **5**, 1634 (1966); *J. Chem. Phys.*, **37**, 2498 (1962); *Can. J. Chem.*, **39**, 318 (1961); (e) J. I. Musher, *Angew. Chem.*, **81**, 68 (1969); (f) K. J. Wynne, "Sulfur Research Trends", Mardi Gras Symposium, 3d, Loyola University, 1971, p 150.

(6) An extensive list of references may be found in the paper by R. Hoffmann, J. M. Howell, and E. L. Muetterties, *J. Am. Chem. Soc.*, **94**, 3047 (1972).

(7) (a) R. D. Willett, *Theor. Chim. Acta*, **2**, 393 (1964); (b) D. P. Santry and G. A. Segal, *J. Chem. Phys.*, **47**, 158 (1967); D. P. Santry, *J. Am. Chem. Soc.*, **90**, 3309 (1968); M. Keeton and D. P. Santry, *Chem. Phys. Lett.*, 7, 105 (1970); (c) R. D. Brown and J. B. Peel, *Aust. J. Chem.*, **21**, 2589, 2605, 2617 (1968); (d) R. M. Gavin, Jr., *J. Chem. Educ.*, **46**, 413 (1969); (e) A. L. Companion, *Theor. Chim. Acta*, **25**, 268 (1970); (f) J. I. Musher and V. B. Koutecky, *ibid.*, **33**, 227 (1974); (g) G. M. Schwenzer and H. F. Schaeffer, III, *J. Am. Chem. Soc.*, **97**, 1391 (1975); L. Radom and H. F. Schaeffer, III, *Aust. J. Chem.*, **28**, 2069 (1975); (h) R. Gleiter and A. Veillard, *Chem. Phys. Lett.*, **37**, 33 (1976); (i) N. Rösch, V. H. Smith, Jr., and M. H. Whangbo, to be published; (j) V. I. Minkin and R. M. Minyaev, *Zh. Org. Khim.*, 11, 1993 (1975); (k) M. Albeck and S. Schaik, *J. Chem. Soc., Perkin Trans. 1*, 1223 (1975).

(8) A detailed discussion of the electronic structure of PH_4 and phosphoranyl radicals in general is given by J. M. Howell, Brooklyn College, to be published. The tetrahedral structure is used as a departure point in this work.

(9) R. Hoffmann, R. W. Alder, and C. F. Wilcox, Jr., *J. Am. Chem. Soc.*, **92**, 4992 (1970).

(10) B. M. Gimarc, *J. Am. Chem. Soc.*, **93**, 593 (1971).

(11) A similar argument has been elegantly applied in a study of the pyramidalization of amines: C. C. Levin, *J. Am. Chem. Soc.*, **97**, 5649 (1975).

(12) R. Hoffmann, *Acc. Chem. Res.*, **4**, 1 (1971); L. Libit and R. Hoffmann, *J. Am. Chem. Soc.*, **96**, 1370 (1974), and references therein.

(13) A comparison should note the difference in the numbering of the levels: $4a_1$ of ref 7g is our $1a_1$, $2b_2$ is our $1b_2$, etc.

(14) L. S. Bartell and R. M. Gavin, Jr., *J. Chem. Phys.*, **48**, 2466 (1968).

(15) (a) R. G. Pearson, *J. Am. Chem. Soc.*, **91**, 4947 (1969); (b) Pearson, on the basis of a different level scheme for SF_4, does find a reason for such a distortion.

(16) O. Foss and K. Maroy, *Acta Chem. Scand.*, **15**, 1945 (1961); O. Foss, K. Maroy and S. Husebye, *ibid.*, **19**, 2361 (1965); K. Fosheim, O. Foss, A. Scheie, and S. Solheimsnes, *ibid.*, **19**, 2336 (1965); O. Foss, H. M. Kjoge, and K. Maroy, *ibid.*, **19**, 2349 (1965), and other work by the same group.

(17) L. S. Bartell and K. W. Hansen, *Inorg. Chem.*, **4**, 1777 (1965); K. W. Hansen and L. S. Bartell, *ibid.*, **4**, 1775 (1965); L. S. Bartell, *ibid.*, **5**, 1635 (1966); L. S. Bartell, *J. Chem. Educ.*, **45**, 754 (1968).

(18) D. R. Johnson and F. X. Powell, *Science*, **164**, 950 (1969).

(19) H. A. Bent, *Chem. Rev.*, **61**, 275 (1961).

(20) A. D. Walsh, *Discuss. Faraday Soc.*, *2*, 18 (1947); *Trans. Faraday Soc.*, **42**, 56 (1946); *ibid.*, **43**, 60, 158 (1947); *Proc. R. Soc. A*, **207**, 13 (1951).

(21) O. Hassel and H. Viervoll, *Acta Chem. Scand.*, 1, 149 (1947); H. J. Dothie, *Acta Crystallogr.*, **6**, 804 (1953); R. E. Marsh, *ibid.*, **8**, 91 (1955).

(22) R. E. Marsh and J. D. McCullough, *J. Am. Chem. Soc.*, **73**, 1106 (1951).

(23) G. C. Demitras and A. G. MacDiarmid, *Inorg. Chem.*, **6**, 1903 (1967).

(24) E. F. Perozzi, J. C. Martin, and I. C. Paul, *J. Am. Chem. Soc.*, **96**, 6735 (1974).

(25) R. Hoffmann, *J. Chem. Phys.*, **39**, 1397 (1963); R. Hoffmann and W. N. Lipscomb, *ibid.*, **36**, 2179, 3489; **37**, 2872 (1962).

The Least-Motion Insertion Reaction $CH_2(^1A_1) + H_2 \rightarrow CH_4$. Theoretical Study of a Process Forbidden by Orbital Symmetry[1a]

Charles W. Bauschlicher, Jr.,[1b] Henry F. Schaefer III,*[1b] and Charles F. Bender[1c]

Contribution from the Department of Chemistry and Lawrence Berkeley Laboratory,[1d] University of California, Berkeley, California 94720, and Lawrence Livermore Laboratory,[1d] University of California, Livermore, California 94550. *Received May 21, 1975*

Abstract: Ab initio electronic structure theory has been applied to the insertion reaction of singlet methylene with molecular hydrogen. Since the molecular orbital descriptions of $CH_2(^1A_1) + H_2$ and CH_4 differ by two electrons, the least-motion approach considered here is forbidden in the sense of Woodward and Hoffmann. Electron correlation was explicitly taken into account via configuration interaction (CI). The CI included all singly and doubly excited configurations (a total of 1192) with respect to three reference configurations. A primary goal was the location of the saddle point or transition state (within the constraints of the least motion approach adopted) geometry with $R = 2.20$ Å, $r = 0.76$ Å, and $\theta = 172°$. This stationary point on the potential energy surface lies 26.7 kcal/mol above separated $CH_2(^1A_1) + H_2$. The portion of the minimum energy path near the saddle point has been obtained by following the gradient of the potential energy in the direction of most negative curvature. The electronic structure at the transition state is compared with that of the reactants and product in terms of the natural orbitals resulting from the wave functions.

In the time since the 1965 publication by Woodward and Hoffmann of their landmark communications,[2] the concept of orbital symmetry has taken on tremendous importance in organic chemistry. The purpose of the present paper is to report a detailed theoretical study of a simple Woodward–Hoffmann forbidden process: the least-motion insertion of singlet methylene into H_2 to yield methane. This pathway is shown qualitatively in Figure 1. There it is seen that C_{2v} symmetry is arbitrarily imposed on the five atoms, whose positions are uniquely defined by the specification of the three geometrical parameters R, r, and θ. An ab initio correlation diagram for

$$CH_2(^1A_1) + H_2(^1\Sigma_g^+) \rightarrow CH_4(^1A_1) \qquad (1)$$

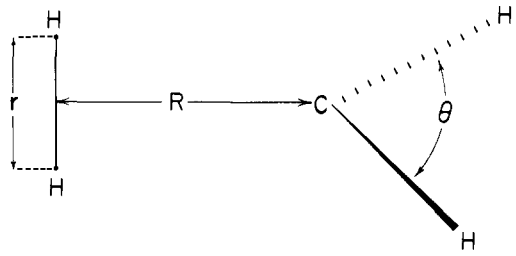

Figure 1. Coordinate system used to describe the least-motion insertion of methylene into hydrogen.

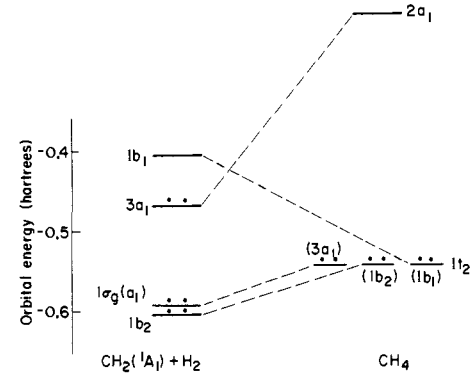

Figure 2. Correlation diagram for the least-motion insertion reaction $CH_2(^1A_1) + H_2 \rightarrow CH_4$.

is given in Figure 2. There it is seen that the wave function for $CH_2(^1A_1) + H_2$ is well described by the single configuration

$$1a_1^2\ 2a_1^2\ 1b_2^2\ 3a_1^2\ 4a_1^2 \qquad (2)$$

while the Hartree–Fock description of methane (after resolution[4] of the T_d orbitals into those of point group C_{2v}) is

$$1a_1^2\ 2a_1^2\ 1b_2^2\ 3a_1^2\ 1b_1^2 \qquad (3)$$

Thus the "forbiddenness" of the least motion insertion is due to the fact that configurations 2 and 3 differ by two electrons. One then expects a large barrier height or activation energy for the process of interest.

This research represents the second step in a comprehensive theoretical study of the reactions of methylene with molecular hydrogen. Our first paper[5a] dealt with the triplet abstraction

$$CH_2(^3B_1) + H_2 \rightarrow CH_3 + H \qquad (4)$$

A large barrier height (15 kcal/mol) was predicted, suggesting that triplet methylene does not react with H_2 in this fashion at room temperature. Since the reactions of CH_2 and H_2 should be analogous to the reactions of CH_2 with saturated hydrocarbons, it is hoped that results obtained for the simpler model system will yield insights of broad applicability.

The first theoretical study of the $CH_2(^1A_1) + H_2$ potential surface appears to be the modified CNDO study of Kollmar.[5b] Other than to establish that the least-motion path (LMP) is *not* the lowest energy pathway, Kollmar paid no special attention to the LMP. However, Kollmar's surface has taken on special significance since its use by Wang and Karplus[6] in one of the first classical trajectory calculations of the dynamics of an organic reaction. Further, Wang and Karplus reported the barrier height for the LMP as 0.021 hartree = 13 kcal/mol. Also pertinent to the present work are two earlier semiempirical studies[7,8] of the potential surface for the more complicated $CH_2(^1A_1) + CH_4 \rightarrow C_2H_6$ insertion reaction.

More recently two ab initio studies of the lowest singlet potential surface of CH_4 have been reported.[9,10] In both the studies of Murrell, Pedley, and Durmaz[9] and of Cremaschi and Simonetta,[10] self-consistent-field (SCF) wave functions were obtained using minimum basis sets. As discussed above, a single-configuration wave function cannot describe the least-motion surface in a continuous manner. However, both of these theoretical studies predict a barrier height in excess of 50 kcal/mol, in qualitative agreement with orbital symmetry arguments.

Theoretical Approach

Perhaps the simplest wave function which can qualitatively describe the least-motion approach of singlet methylene to hydrogen to yield methane includes the two configurations 2 and 3. Our calculations actually begin with a three-configuration SCF wave function, including (2) and (3), plus

$$1a_1^2\ 2a_1\ {}^23a_1^2\ 4a_1^2\ 1b_1^2 \qquad (5)$$

This optimum three-configuration wave function was obtained by the annihilation[11,12] of all singly excited configurations with respect to the three reference determinants (2), (3), and (5). The basis set chosen was of the contracted Gaussian double ζ type, as described fully in our earlier methylene studies.[5a,11,13]

Following the SCF calculations, configuration interaction was carried out including all (except, as usual, that the $1a_1$ core orbital was always held doubly occupied) single and double excitations with respect to the three reference states. This amounts to a total of 1192 $^1A_1$ configurations, consistent with our goal[5a,11,13] of at least 90% of the valence shell correlation energy attainable within the chosen basis set. We note that restriction of the calculations to the least-motion path allows us to maintain C_{2v} symmetry everywhere. The iterative natural orbital procedure[14] was used to guarantee a nearly optimum set of orbitals for the multiconfiguration calculations. The natural orbitals also allow a simple interpretation of these relatively complicated wave functions.

As mentioned in the introductory section, Figure 1 gives the coordinate system used herein. In all calculations the methylene C–H distance was taken to be 2.06 bohrs = 1.090 Å. For $^1A_1$ CH_2, r_0(CH) has been determined experimentally[4] to be 1.11 Å, while for the product CH_4 molecule r_0(CH) = 1.094 Å. Thus it is reasonable to assume relatively little variation in this CH separation during the reaction.

The remaining three geometrical parameters have been varied to emphasize the saddle point region. R, the separa-

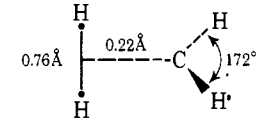

tion between the C atom and the H_2 midpoint, takes on the values 5.00, 4.50, 4.25, 4.00, 3.75, 3.50, 3.25, 3.00, and 2.75 bohrs. The H–H separation r was 1.3, 1.4, 1.5, 1.6, 1.7, and 1.8 bohrs. Finally, a large range of methylene angles θ was considered: 100, 110, 120, 130, 140 , 150, 160, 170, 180°. Thus a total of ~500 points on the potential surface was computed.

Using a separation of R = 100, the bond angle of singlet methylene was predicted to be 106.5°, compared to experiment[4] of 102.4°. The same calculations yield an H–H separation for H_2 of 1.409 bohrs, as opposed to experiment 0.7414 Å = 1.401 bohrs.[15] The total energy of $CH_2 + H_2$ obtained from these CI calculations is −40.0951 hartrees.

For CH_4, no geometry optimization is required, as the tetrahedral bond angle 109°28′ and methylene CH distance of 2.06 bohrs fully specify the geometry. At this CH_4 geometry the total energy is −40.2947 hartrees. Thus the exothermicity for $CH_2 + H_2 \rightarrow CH_4$ is 0.1996 hartree or 125.2 kcal/mol. This may be compared with the best available value, 122 kcal/mol. This experimental result is obtained by adding a theoretical $^3B_1 - {}^1A_1$ separation[17] of 14 kcal/mol to the known value[16] of 108 ± 1 kcal/mol for the ground state process $CH_2 + H_2 \rightarrow CH_4$.

Barrier Height and Saddle Point Geometry

Given the potential energy computed at the geometries stated above, the general vicinity of the saddle point was located visually. Then the surface in that region was fit to a three-dimensional spline function, which is guaranteed to precisely fit each computed point. Given this form for the surface, the saddle point or transition state was located as the point at which the gradient of the potential energy was zero.

The predicted barrier height is 26.75 kcal/mol, significantly higher than the 13 kcal/mol reported[6] for Kollmar's semiempirical surface, but much lower than previous ab initio surfaces.[9,10] Although it is difficult to estimate the accuracy of our barrier prediction (or of Kollmar's for that matter), previous comparisons[18-20] with experiment and more accurate theoretical treatments suggest an error range of +3 to −7 kcal/mol. Such a large barrier (20-30 kcal/mol) is certainly consistent with the Woodward-Hoffmann forbiddenness of the least motion path. If the LMP were in fact the lowest energy pathway on the entire surface, the reaction would not occur at all under normal laboratory conditions. However, as we will show in a later paper,[21] the true minimum energy path is of lower symmetry than the C_{2v} LMP discussed here.

The saddle point occurs at R = 4.155 bohrs, θ = 172.4°, r = 1.429 bohrs. The R and r values are as expected, since the transition state for such a highly exothermic reaction is expected to resemble the reactants.[22] However, the methylene bond angle at the saddle point is much larger than that for either the reactants (106.5°) or products (109.5°). Here we must keep in mind, however, that our constrained transition state is not[6-8] the true unrestricted transition state for the insertion reaction. Hence Hammond's theorem probably should not be applied at all in the case of the present highly constrained potential surface.

This qualitatively surprising result certainly requires some explanation. The simplest reasonable explanation takes notice of the fact that the expected least-motion approach necessitates a very high electron density in the triangle connecting the C atom and H_2 nuclei. This is illustrated in the simple visualization seen below.

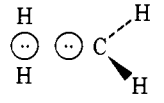

(6)

Since there is little freedom available (in our constrained least motion approach) to the H_2 electron distribution, the easiest way to avoid this unfortunate circumstance (having four electrons localized in a specific region of space) is to somehow perturb the singlet methylene lone pair. In hindsight, the way to accomplish this is obvious; when singlet methylene is bent away from its equilibrium bond angle (106.5°) to a linear geometry, the lone pair is no longer localized but instead free to "rotate" about the axis of the linear molecule. In less intuitive but more palatable language, the orbital in question takes on a cylindrical electron density. In any case, this unusual constrained transition state

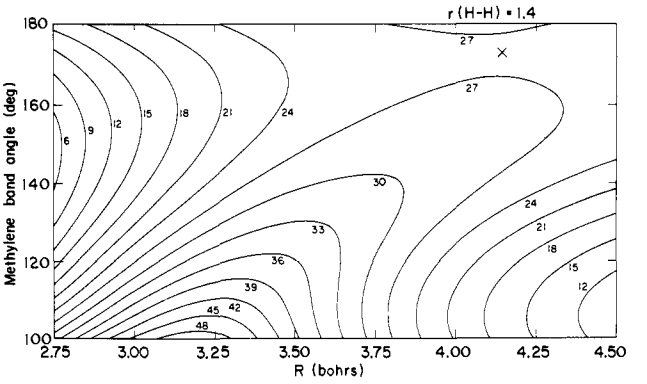

Figure 3. Contour map for the least-motion approach of $CH_2(^1A_1)$ to H_2 for fixed r(H-H) = 1.4 bohrs. Contours are labeled in kcal/mol relative to infinitely separated $CH_2(^1A_1) + H_2$. The saddle point position is marked by an X.

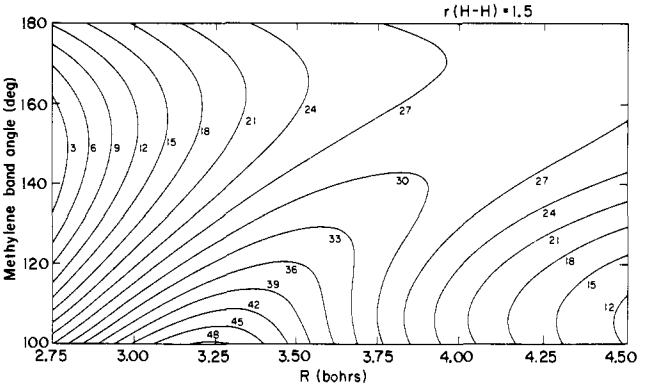

Figure 4. Same as Figure 3, except that r(H-H) = 1.5 bohrs.

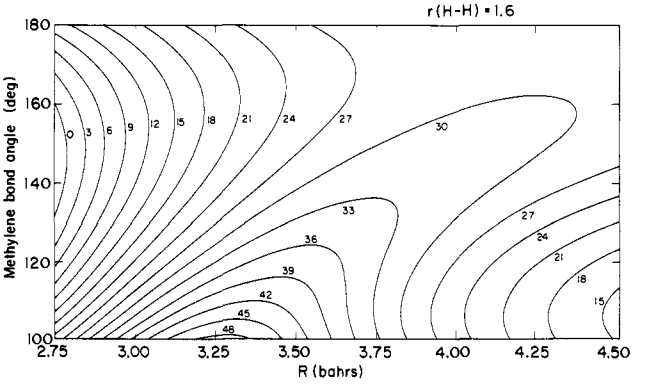

Figure 5. Same as Figure 3, except that r(H-H) = 1.6 bohrs.

may be qualitatively understood as a means of escape from the unfavorable interaction of the singlet methylene lone pair with the doubly occupied $1\sigma_g$ orbital of H_2.

Overview of the Surface

We have found one of the most understandable ways of looking at the least motion $CH_2(^1A_1) + H_2 \rightarrow CH_4$ surface to be in terms of contour maps which set the parameter r equal to a fixed value. In Figures 3, 4, 5, and 6, these contours are presented for H-H separations of r = 1.4, 1.5, 1.6, and 1.7 bohrs. Since the saddle point occurs at r = 1.429 bohrs, it is clear that Figure 3 gives us the closest view of the transition state region. An even closer view of this region is given in Figure 8, which utilizes additional points on the surface (specifically R = 3.875 bohrs).

Comparison of Figures 3-6 is especially interesting since the qualitative effects of stretching the H_2 bond are illus-

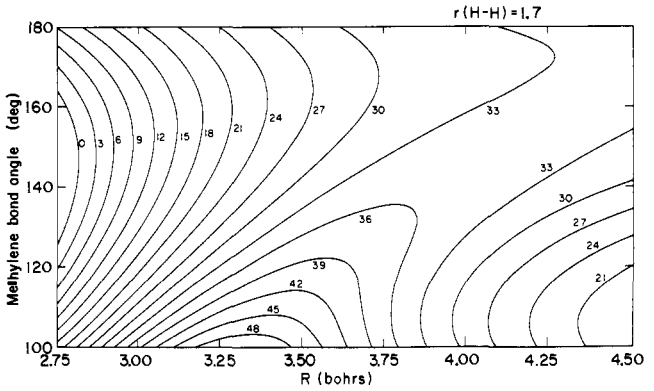

Figure 6. Same as Figure 3, except that r(H-H) = 1.7 bohrs.

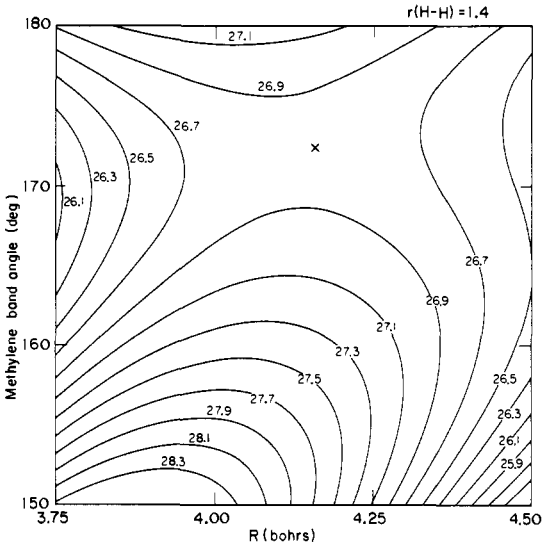

Figure 7. Relatively close-up view of the potential surface in the region surrounding the saddle point. Contours are labeled in kcal/mol relative to separated $CH_2(^1A_1)$ + H_2. The saddle point position is marked by an ×.

trated. First, the barrier becomes progressively larger as r increases from 1.4 bohrs. Second, the attractive part of the surface becomes more apparent for the larger r values. For example, at r = 1.7 bohrs, the E = 0 kcal/mol contour is apparent at the left edge of Figure 7. The lowest comparable contour for r = 1.4, on the other hand, is E = 6 kcal/mol. It is to be emphasized, of course, that the present study does not give a complete picture of the CH_4 surface. Our largest r value is 1.7, while in the isolated methane molecule this distance is 3.364 bohrs.

Reaction Pathways

In two recent papers[5a,23] we have discussed in some detail the relationships between different types of reaction pathways. Traditionally, one chooses a "reaction coordinate" (R is the perhaps most obvious choice for the present system) and minimizes the total energy with respect to all other geometrical parameters. Unfortunately the pathway defined in this way is often discontinuous. That this is the case for $CH_2(^1A_1) + H_2 \rightarrow CH_4$ is seen clearly in Figure 8. At $R \sim$ 3.8 bohrs along the reaction coordinate, the optimum value of θ changes discontinuously from ~105° to ~107°.

A more acceptable reaction pathway is found by first locating the saddle point and then following the gradient of the potential energy in the direction of steepest descent. We refer to the pathway thus mapped out as the minimum energy path. Although this procedure is much to be preferred over the "reaction coordinate" approach, it has the disadvantage that the gradient and hence the pathway are dependent on the chosen coordinate. To overcome this difficulty we have used a coordinate invariant minimum energy path,[23] in which a large number of small states (again fol-

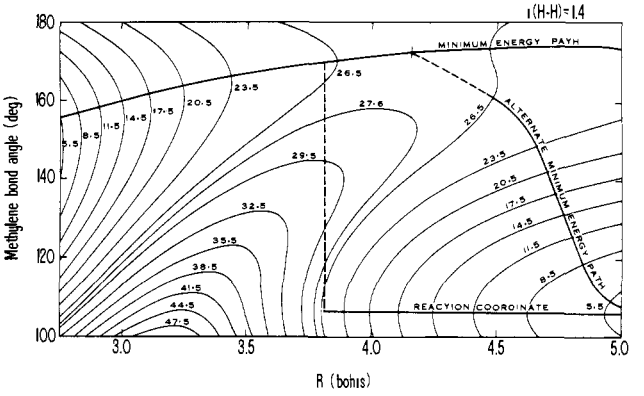

Figure 8. Contour map (with r(H-H) = 1.4 bohrs) used to illustrate several types of pathways for the singlet methylene insertion reaction. The saddle point position is marked by a vertical line through the minimum energy path. The alternate minimum-energy path begins with the 26.5 kcal/mol contour.

Table I. Coordinate Invariant Minimum Energy Path for $CH_2(^1A_1)$ + $H_2 \rightarrow CH_4$[a]

R, bohrs	θ, deg	r, bohrs	E, kcal/mol	
∞	106.5	1.41	0.0	Reactants
5.0	172.9	1.42	25.4	
4.9	174.0	1.42	25.6	
4.8	174.2	1.42	25.8	
4.7	174.0	1.42	26.0	
4.6	173.7	1.42	26.2	
4.5	173.4	1.42	26.4	
4.4	173.0	1.42	26.6	
4.3	172.7	1.42	26.7	
4.155	172.4	1.43	26.75	Saddle point
4.0	171.4	1.44	26.6	
3.9	170.6	1.44	26.4	
3.8	169.8	1.45	25.9	
3.7	168.9	1.45	25.5	
3.6	167.9	1.46	24.7	
3.5	166.8	1.48	23.6	
3.4	165.6	1.50	22.2	
3.3	164.4	1.52	20.2	
3.2	163.0	1.55	17.7	
3.1	161.5	1.57	14.7	
3.0	159.7	1.62	10.8	
2.9	158.3	1.67	6.0	
2.85	157.5	1.69	3.2	
1.19	109.5	3.36	−125.2	Products

[a] See Figure 1 for the coordinate system used. Energies are given relative to the separated reactants.

Table II. Alternate Minimum Energy Path for the Region 4.4 < R < ∞[a]

R, bohrs	θ, deg	r, bohrs	E, kcal/mol	
∞	106.5	1.41	0.0	Reactants
5.0	107.8	1.41	5.1	
4.9	113.1	1.41	6.5	
4.8	125.5	1.41	11.7	
4.7	144.5	1.41	21.8	
4.6	156.2	1.42	25.7	
4.5	160.6	1.42	26.4	

[a] As discussed in the text, this pathway is more dynamically realistic than the comparable portion shown in Table I. Format is as in Table I.

Table III. Configurations with Coefficient $\geq 0.0447 = (0.002)^{1/2}$ in the CI Wave Functions for Three Points on the $CH_2(^1A_1) + H_2 \rightarrow CH_4$ Potential Surface[a]

Reactants		Saddle Point		Products	
$2a_1^2\ 1b_2^2\ 3a_1^2\ 4a_1^2$	0.9137	$2a_1^2\ 1b_2^2\ 3a_1^2\ 1b_1^2$	0.8204	$2a_1^2\ 1b_2^2\ 3a_1^2\ 1b_1^2$	0.9500
$2a_1^2\ 1b_2^2\ 3a_1^2\ 1b_1^2$	0.0390	$2a_1^2\ 1b_2^2\ 3a_1^2\ 4a_1^2$	0.1294	$2a_1^2\ 1b_2\ 3a_1\ 1b_1^2\ 2b_2\ 4a_1$	0.0042
$2a_1^2\ 1b_2^2\ 4a_1^2\ 2b_1^2$	0.0101	$2a_1^2\ 1b_2^2\ 3a_1^2\ 2b_1^2$	0.0044	$2a_1^2\ 3a_1^2\ 1b_1^2\ 2b_2^2$	0.0040
$2a_1^2\ 3a_1^2\ 4a_1^2\ 2b_2^2$	0.0040	$2a_1^2\ 1b_2\ 3a_1^2\ 1b_1\ 2b_2\ 2b_1$	0.0039	$2a_1^2\ 1b_2^2\ 3a_1^2\ 2b_1^2$	0.0040
$2a_1\ 1b_2\ 3a_1^2\ 4a_1^2\ 5a_1\ 2b_2$	0.0040	$2a_1^2\ 1b_2^2\ 1b_1^2\ 3b_1^2$	0.0032	$2a_1\ 1b_2^2\ 3a_1^2\ 1b_1\ 2b_1\ 5a_1$	0.0033
$2a_1^2\ 1b_2\ 3a_1^2\ 4a_1\ 5a_1\ 2b_2$	0.0023	$2a_1\ 1b_2^2\ 3a_1^2\ 1b_1\ 2b_1\ 7a_1$	0.0026	$2a_1^2\ 1b_2^2\ 3a_1\ 1b_1\ 4a_1\ 2b_1$	0.0032
$2a_1^2\ 1b_2^2\ 3a_1^2\ 6a_1^2$	0.0021	$2a_1^2\ 1b_2^2\ 1b_1^2\ 3b_1\ 4b_1$	0.0025	$2a_1\ 1b_2\ 3a_1^2\ 1b_1^2\ 2b_2\ 5a_1$	0.0030
$1b_2^2\ 3a_1^2\ 4a_1^2\ 5a_1^2$	0.0021	$2a_1^2\ 3a_1^2\ 1b_1^2\ 6a_1^2$	0.0024	$2a_1\ 1b_2^2\ 3a_1\ 1b_1^2\ 4a_1\ 5a_1$	0.0029
$2a_1^2\ 1b_2^2\ 4a_1^2\ 7a_1^2$	0.0020			$2a_1^2\ 1b_2^2\ 1b_1^2\ 4a_1^2$	0.0021

[a] Note that $\Sigma_i C_i^2 = 1$, and the C_i^2 are reported here.

lowing the gradient) is taken, but the inertia tensor is diagonalized prior to each step. This coordinate invariant pathway is simply labeled "minimum energy path" in Figure 8 and is reported in more detail in Table I. It is seen that the three geometrical parameters vary smoothly in going from reactants to products. Recall that a three-dimensional spline representation[24] of the potential surface was used to compute the gradient at each desired point. An analysis of this procedure will be reported in the thesis of one of us (C.W.B.).

Although the minimum energy path seen in Figure 8 and Table I is nicely continuous, it is quite unlikely that a classical trajectory carried out for our constrained system would come close to this pathway. This conclusion is based on the very slow decrease in the bond angle θ between the saddle point ($R = 4.15$ bohrs) and $R = 5.0$. Our feeling is that singlet methylene approaching at such a large separation from hydrogen is extremely unlikely to have a bond angle of 170° Closer inspection of Figure 8 shows that the reason for this dynamically unrealistic pathway is the unusual shape of the 26.5 kcal/mol contour. This contour in effect "pushes" the minimum energy path into its large angle course. However, with a negligible additional amount of energy, one can follow the "alternate" minimum energy path labeled thus in Figure 8. This path was generated by the same coordinate invariant procedure described above, but beginning at the contour labeled 26.5 kcal/mol. Table II shows the alternate path in detail.

Our general conclusion concerning these various pathways is that it is very important to have actual contour maps available when discussing a potential surface. Any single pathway, no matter how carefully and mathematically correctly constructed, can sometimes give a misleading picture of the reaction.

Electronic Structure Considerations

One of our primary concerns here is with electronic structure changes accompanying a Woodward-Hoffmann forbidden process. Therefore we have attempted to compare the correlated wave functions at the saddle point with those of the reactants and products. In this spirit, Table III compares the important configuration in the three wave functions and Table IV the natural orbital occupation numbers.

The primary conclusion to be drawn from Tables III and IV is that the electronic structure of the transition state resembles CH_4 much more closely than $CH_2(^1A_1) + H_2$. Here it is illuminating to recall that, in accord with Hammond's postulate,[22] the opposite is true for the transition state geometry. Note that the configuration 3, which represents 95% of the CI wave function for methane, corresponds to 82% of the transition state wave function. Configuration 2, representing 91% of the $CH_2 + H_2$ wave function, contributes only 13% to the transition state. The same conclusion may be reached through inspection of the natural orbital occupation numbers, which show both the $1b_1$ (1.71 "electrons") and $4a_1$ (0.28) orbitals to be significantly populated. Comparison with reactants and products clearly implies that electron correlation is more important at the saddle point than at either of the two end points. This may also be seen in the rather large barrier heights (>50 kcal/mol) predicted in previous studies[9,10] neglecting correlation effects.

Table IV. Natural Orbital Occupation Numbers from the 1192 Configuration Wave Functions for $CH_2(^1A_1) + H_2 \rightarrow CH_4$

Orbital	$CH_2(^1A_1) + H_2$	Saddle point	CH_4
$1a_1$	2.0000	2.0000	2.0000
$2a_1$	1.9783	1.9791	1.9834
$3a_1$	1.9745	1.9718	1.9721
$4a_1$	1.8982	0.2751	0.0211
$5a_1$	0.0202	0.0220	0.0180
$6a_1$	0.0126	0.0051	0.0053
$7a_1$	0.0042	0.0037	0.0026
$8a_1$	0.0032	0.0026	0.0006
$9a_1$	0.0003	0.0004	0.0002
$10a_1$	2×10^{-6}	2×10^{-6}	1×10^{-6}
$1b_1$	0.0859	1.7079	1.9722
$2b_1$	0.0210	0.0245	0.0204
$3b_1$	0.0010	0.0159	0.0053
$4b_1$	0.0002	0.0005	0.0005
$1b_2$	1.9729	1.9735	1.9720
$2b_2$	0.0225	0.0153	0.0205
$3b_2$	0.0041	0.0023	0.0053
$4b_2$	0.0007	0.0001	0.0005

References and Notes

(1) (a) Supported in part by the National Science Foundation, Grant GP-41509X. (b) University of California, Berkeley. (c) University of California, Livermore. (d) Work performed under the auspices of the U.S. Energy Research and Development Administration.

(2) R. B. Woodward and R. Hoffmann, *J. Am. Chem. Soc.*, **87**, 395, 2046, 2511 (1965). See also R. B. Woodward and R. Hoffmann, "The Conservation of Orbital Symmetry", Verlag Chemie, Weinheim/Bergstr., Germany, 1970. This process is also unfavored according to the orbital phase continuity principle, W. A. Goddard, *J. Am. Chem. Soc.*, **94**, 793 (1972).

(3) This correlation diagram employs orbital energies obtained from ab initio calculations on CH_2, H_2, and CH_4. We thank Mr. Steven R. Ungemach for the use of his unpublished results.

(4) G. Herzberg, "Electronic Spectra of Polyatomic Molecules", Van Nostrand-Reinhold, New York, N.Y., 1966.

(5) (a) C. P. Baskin, C. F. Bender, C. W. Bauschlicher, and H. F. Schaefer, *J. Am. Chem. Soc.*, **96**, 2709 (1974); (b) H. Kollmar, *Tetrahedron*, **28**, 5893 (1972).

(6) I. S. Y. Wang and M. Karplus, *J. Am. Chem. Soc.*, **95**, 8160 (1973).

(7) R. C. Dobson, D. M. Hayes, and R. Hoffmann, *J. Am. Chem. Soc.*, **93**, 6188 (1971).

(8) N. Bodor, M. J. S. Dewar, and J. S. Wasson, *J. Am. Chem. Soc.*, **94**, 9095 (1972).

(9) J. N. Murrell, J. B. Pedley, and S. Durmaz, *J. Chem. Soc., Faraday Trans. 2*, **69**, 1370 (1973).

(10) P. Cremaschi and M. Simonetta, *J. Chem. Soc., Faraday Trans. 2*, **70**, 1801 (1974).

(11) C. F. Bender and H. F. Schaefer, *J. Am. Chem. Soc.*, **92**, 4984 (1970).
(12) G. M. Schwenzer, S. V. O'Neil, H. F. Schaefer, C. P. Baskin, and C. F. Bender, *J. Chem. Phys.*, **60**, 2787 (1974).
(13) S. V. O'Neil, H. F. Schaefer, and C. F. Bender, *J. Chem. Phys.*, **55**, 162 (1971).
(14) C. F. Bender and E. R. Davidson, *J. Phys. Chem.*, **70**, 2675 (1966).
(15) B. Rosen, "Spectroscopic Data Relative to Diatomic Molecules", Pergamon Press, Oxford, 1970.
(16) D. R. Stull and H. Prophet, JANAF Thermochemical Tables, 2nd ed, National Bureau of Standards, Washington, D.C., 1971.
(17) (a) C. F. Bender, H. F. Schaefer, D. R. Franceschetti, and L. C. Allen, *J. Am. Chem. Soc.*, **94**, 6888 (1972); (b) P. J. Hay, W. J. Hunt, and W. A. Goddard, *Chem. Phys. Lett.*, **13**, 30 (1972); (c) J. F. Harrison, *Acc. Chem. Res.*, **7**, 378 (1974); (d) V. Staemmler, *Theor. Chim. Acta*, **35**, 309 (1974); (e) for an experimentally based discussion of the singlet–triplet separation, see H. M. Frey and G. J. Kennedy, *J. Chem. Soc., Chem. Commun.*, 233 (1975).
(18) C. F. Bender, P. K. Pearson, S. V. O'Neil, and H. F. Schaefer, *J. Chem. Phys.*, **56**, 4626 (1972).
(19) S. V. O'Neil, P. K. Pearson, H. F. Schaefer, and C. F. Bender, *J. Chem. Phys.*, **58**, 1126 (1973).
(20) S. V. O'Neil, H. F. Schaefer, and C. F. Bender, *Proc. Natl. Acad. Sci. U.S.A.*, **71**, 104 (1974).
(21) C. W. Bauschlicher, H. F. Schaefer, and C. F. Bender, research in progress.
(22) G. S. Hammond, *J. Am. Chem. Soc.*, **77**, 334 (1955).
(23) H. F. Schaefer, *Chem. Br.*, 11, 227 (1975).
(24) C. W. Bauschlicher, unpublished work.

Molecular Structure of the ClF_2 and ClF_4 Radicals. A Theoretical Study[1]

Steven R. Ungemach and Henry F. Schaefer III*

Contribution from the Department of Chemistry and Lawrence Berkeley Laboratory, University of California, Berkeley, California 94720. *Received July 2, 1975*

Abstract: ClF_2 and ClF_4 are two interesting inorganic radicals whose quantitative molecular structures have not been determined experimentally. A priori electronic structure theory has been used in the present research to predict the structures of these radicals and their positive and negative ions. Self-consistent-field theory has been employed in conjunction with both minimum and double ζ basis sets. For ClF_2 more extended basis sets were used in addition. The ClF_2^+ ion has a bent (bond angle 97.4°) structure quite similar to that of the isoelectronic SF_2 molecule, while ClF_2^- is linear. ClF_2 is predicted C_{2v} with bond length 1.72 Å and bond angle near 148°. Both minimum and double ζ basis sets predict ClF_4^+ to be square pyramidal, in contrast with the known stucture of the isoelectronic SF_4 molecule. Finally, both ClF_4 and ClF_4^- are predicted to be planar. However, these structural predictions are qualitatively altered when chlorine 3d functions are added to the basis set. Electronic structures are discussed in terms of orbital energies and Mulliken populations.

For some time now the interhalogen compounds have been known to have a rich and interesting chemistry.[2,3] However, for the most part, this chemistry has been limited to molecules with closed-shell ground states, hence an even number of electrons. For example, consider the chlorine fluorides ClF_n, which are the subject of the present research. Of these, the even-electron molecules ClF, ClF_3, and ClF_5 are long-lived at room temperature and have at least reasonably well-defined physical properties.[3] Moreover, the structures of all three are known. ClF has a bond distance of 1.628 Å and a dipole moment of 0.88 A (Cl^+F^-).[4,5] ClF_3 has a dipole moment of 0.56 D[6] and is a planar T-shaped molecule[7]

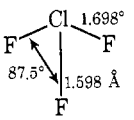

(1)

Although less precisely determined, the shape of ClF_5 is thought to be a square pyramid,[8] with apical and basal Cl–F bond distances of 1.62 and 1.72 Å.

In contrast, relatively little is known about interhalogens with an odd number of electrons. In fact, in their recent review Downs and Adams[3] indicate, except for two or three reported observations, "interhalogen radicals are the subject more of speculation than of first-hand evidence". Of specific interest here are the ClF_2 and ClF_4 radicals. ClF_2 was first prepared by Mamantov and coworkers,[9] who have assigned the vibrational frequencies[10] ν_1 = 536 cm^{-1} (symmetric stretch), ν_2 = 242 cm^{-1} (bending), and $\nu_3 \sim$ 575 cm^{-1} (asymmetric stretch). Based on their assignments Mamantov et al. determined the ClF_2 bond angle to be 136 ± 15° or 144 ± 15°, depending on whether they used computer-simulated or observed frequencies. In any case, their final result of 140 ± 19° implies a measurably bent triatomic molecule. This result is of particular interest since it contrasts with Nelson and Pimentel's conclusion,[11] also based on matrix isolation spectroscopy, that the related Cl_3 radical is linear. It should also be noted that ClF_2 has been hypothesized as an intermediate in a number of chemical reactions, and a value of the heat of formation, −19 ± 2 kcal/mol, has been determined.[12]

Our initial interest in ClF_2 and ClF_4 was due to the proposal of Krogh and Pimentel[13] that the $H_2 + ClF_3$ system might yield a chain-branching chemical laser. Their proposal[13] led to an interesting exchange between Suchard[14] and Pimentel,[15] and in turn to molecular beam[16] and flow system[17] studies of the $H + ClF_3 \rightarrow HF + ClF_2$ reaction. While the flow experiments give no evidence of product HF at mean collision energies of 1–2 kcal/mol, the beam experiments (carried out at ~10 kcal/mol collision energy) do yield HF as an observable product.

Quite recently, Morton and Preston have detected ClF_4 as a product in the fluorination of Cl_2 or HCl by hypofluorite photolysis.[18] Based on the observed ESR spectrum, Morton and Preston concluded that ClF_4 is a planar molecule belonging to the point group D_{4h} and having a $^2A_{1g}$ ground electronic state. Semiempirical theoretical studies of ClF_4 have been reported by Gregory.[19] Using several variants of the CNDO and INDO schemes, Gregory in each case predicts ClF_4 to be planar or slightly nonplanar with a very small (1–4 cm^{-1}) inversion barrier.

There have been a number of experimental studies of the positive and negative ions of ClF_2 and ClF_4. Both the ClF_2^+ and ClF_2^- ions have been observed experimentally by Christe and co-workers.[20,21] Based on the infrared and